Title	Status of neutron spectrometers at J-PARC
Author(s)	Kajimoto Ryoichi, Yokoo Tetsuya, Nakamura Mitsutaka, Kawakita Yukinobu, Matsuura Masato, Endo Hitoshi, Seto Hideki, Ito Shinichi, Nakajima Kenji, Kawamura Seiko
Citation	Physica B: Condensed Matter,562,p.148-154
Text Version	Accepted Manuscript
URL	https://jopss.jaea.go.jp/search/servlet/search?5063092
DOI	https://doi.org/10.1016/j.physb.2018.11.061
Right	© 2019 This manuscript version is made available under the CC-BY-NC-ND 4.0 license http://creativecommons.org/licenses/by-nc-nd/4.0/

Status of neutron spectrometers at J-PARC

Ryoichi Kajimoto[a,*], Tetsuya Yokoo[a,b], Mitsutaka Nakamura[a], Yukinobu Kawakita[a], Masato Matsuura[c], Hitoshi Endo[a,b], Hideki Seto[a,b], Shinichi Itoh[a,b], Kenji Nakajima[a], Seiko Ohira-Kawamura[a]

[a] *Materials and Life Science Division, J-PARC Center, Tokai, Ibaraki 319-1195, Japan*
[b] *Institute of Materials Structure Science, High Energy Accelerator Research Organization (KEK), Tsukuba, Ibaraki 305-0801, Japan*
[c] *Neutron Science and Technology Center, Comprehensive Research Organization for Science and Society (CROSS), Tokai, Ibaraki 319-1106, Japan*

Abstract

Seven time-of-flight quasielastic/inelastic neutron scattering instruments are installed on six beamlines in the Materials and Life Science Experimental Facility (MLF) at the Japan Proton Accelerator Research Complex (J-PARC). Four of these instruments are chopper-type direct-geometry spectrometers, one is a near-backscattering indirect-geometry spectrometer, and the other two are spin-echo-type spectrometers. This paper reviews the characteristic features, recent scientific outcomes, and progress in development of MLF spectrometers.

Keywords: J-PARC, Materials and Life Science Experimental Facility, Quasielastic neutron scattering, Inelastic neutron scattering

1. Introduction

The Materials and Life Science Experimental Facility (MLF) at the Japan Proton Accelerator Research Complex (J-PARC) is a 1-MW-class spallation neutron and muon source. The neutron source consists of a liquid mercury target and supercritical hydrogen moderators [1]. The first neutron beam was produced on May 30, 2008. Since then, the beam power has increased gradually, and the beam power was 500 kW as of June, 2018. The MLF houses 23 neutron beamlines [2], of which 21 are occupied by time-of-flight (TOF) neutron scattering instruments. Six beamlines are quasielastic neutron scattering (QENS) or inelastic neutron scattering (INS) beamlines, and they constitute the MLF Spectroscopy Group [2, 3].

Fig. 1 shows the momentum (Q) and energy (E) range that can be accessed by the MLF spectrometers [3]. 4SEASONS, HRC, AMATERAS, and POLANO are direct-geometry spectrometers; 4SEASONS is a thermal neutron chopper spectrometer covering the range of 10^0–10^2 meV [4]. HRC can access higher energies [5], while AMATERAS is optimized for lower energies [6]. POLANO has the capability to use polarized neutrons [7]. By contrast, DNA is a near-back scattering spectrometer with a pulse-shaping chopper [8]. Measurements with μeV resolution can be performed using this instrument. VIN ROSE consists of two neutron spin echo spectrometers, MIEZE and NRSE, and it can access even slower dynamics [9]. 4SEASONS, HRC, and AMATERAS have been open to users before the other instruments were, followed by DNA. The user program of VIN ROSE was started recently with a part of its instrument suite, while on-beam commissioning has started in the case of POLANO. Various combinations of these instruments at MLF facilitate studies on dynamics in wide range of fields, including solid-state physics, amorphous materials and liquids, soft and biological matters, as well as industrial applications such as tire rubbers and battery materials.

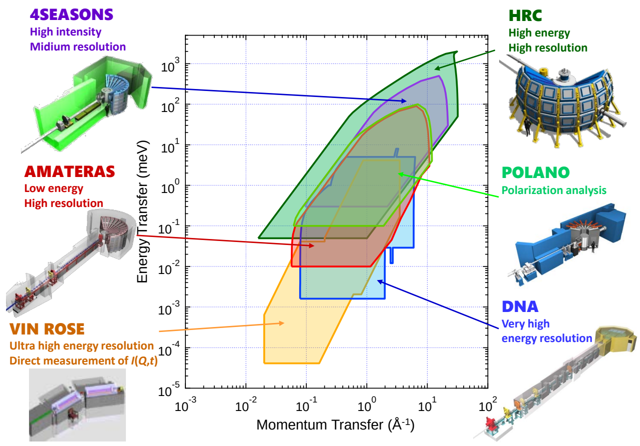

Figure 1: MLF spectrometers and their coverages in momentum-energy space [3].

In this paper, we review the recent status of the six spectrometers. In Section 2, recent scientific results obtained using the MLF spectrometers, as well as characteristic features of the instruments that led to these results, are overviewed. Section 3 describes recent progress in instrument development of the MLF spectrometers. Section 4 presents the results of experiments performed with 1 MW beam power on July 2018 to demonstrate instrument performance in the final phase of the facility. Finally, Section 5 summarizes the present study. The specifications and parameters of the instruments are summarized in Refs. [2, 3].

*Corresponding author
Email address: `ryoichi.kajimoto@j-parc.jp` (Ryoichi Kajimoto)

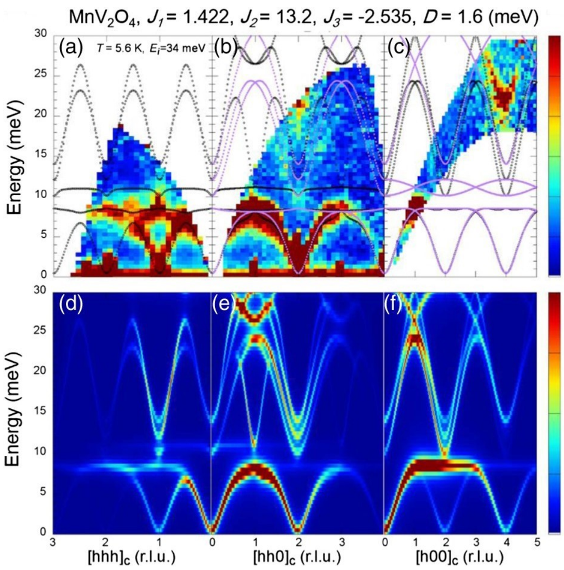

Figure 2: Inelastic scattering intensity of MnV_2O_4 along (a) $[hhh]_c$, (b) $[hh0]_c$, and (c) $[h00]_c$ directions observed at 5.6 K by using 4SEASONS. (d)–(f) Calculated intensity contours corresponding to (a)–(c). The purple and black dots are the calculated spin-wave dispersions along the $[h0h]$ and the $[hh0]$ directions in (b) and along the $[00l]$ and $[h00]$ directions in (c), respectively. The figure is reproduced from Ref. [13].

2. Results obtained using MLF spectrometers

2.1. 4SEASONS

4SEASONS is capable of highly efficient measurements at moderate resolutions in the energy range of up to ∼300 meV. Observations of the full spectra of two-dimensional (2D) magnetic excitations in copper- and iron-based superconductors have yielded typical outcomes (For example, see Refs. [10–12]). In addition, a number of experiments involving mapping full excitation spectra in a four-dimensional (4D) $\boldsymbol{Q}$-E space with rotating single crystals have been conducted [13, 14]. Figs. 2(a)–(c) show the magnetic excitation spectra of the spinel-type vanadium oxide MnV_2O_4 along the primary axes of the cubic lattice [13]. This compound shows ordering of orbitals and spins, and coupling between the orbital and the spin degrees of freedom is expected. The 4D excitation spectra were obtained by many inelastic scattering spectra rotating the crystal in steps of 0.5° and reconstructing the obtained spectra into a 4D matrix of $\boldsymbol{Q}$, E, and intensity [15]. The dots represent the spin-wave dispersions calculated using a Heisenberg model that considers twinning of the crystal. Figs. 2(d)–(f) show the calculated intensity contours corresponding to Figs. 2(a)–(c). Most of the observed spectra are reproduced by the calculation instead of the scatterings around 20 meV in Figs. 2(b) and 2(c). Matsuura et al. argued that the latter scatterings originated from the spin-orbital coupled excitation [13]. To further improve the measurement efficiency of 4D mapping measurements, the 4SEASONS group in collaboration with the MLF Computing Environment Group developed a new measurement system, which collects data by rotating single crystals continuously and visualizes the collected data in real-time [16, 17].

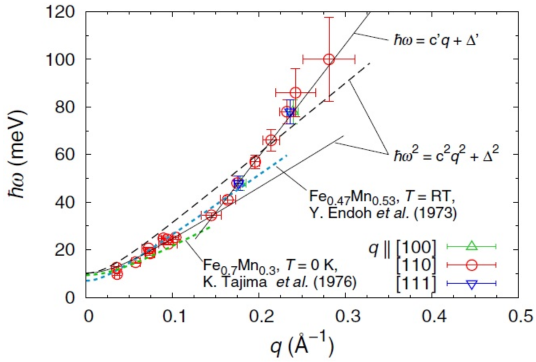

Figure 3: Dispersion relation of spin-wave excitations in $Fe_{0.7}Mn_{0.3}$ observed at 14 K by using HRC. The black dashed and solid curves show fits with $E^2 = c^2q^2 + \Delta^2$. The black solid straight line shows a linear fit. The green and blue dashed curves show previously reported dispersion relations. The figure is reproduced from [19].

2.2. HRC

HRC combines INS with a wide energy range and high resolution. High-resolution experiments in conventional energy-momentum spaces have produced many outcomes in condensed matter physics, especially in the field of magnetism (for example, see Ref. [18–20]). Fig. 3 shows the dispersion relation of the spin-wave excitations in the itinerant antiferromagnet $Fe_{0.7}Mn_{0.3}$ observed by Ibuka et al. [19]. Magnetic excitations in itinerant antiferromagnets have been studied since a long time ago, but the mechanism of these magnetic excitations remains debated. Ibuka et al. observed the spin-wave excitations in a single crystal of this material at energies of up to E = 100 meV by employing incident energies (E_is) as high as 372 meV. They found that the spin-wave velocity increases suddenly at 40 meV, and the damping parameter of the spin-wave increases at energies higher than 40 meV. This finding suggests that the spin-wave excitations merge with the continuum of the individual particle-hole excitations at 40 meV.

The combination of high resolution and high energy can mitigate the kinematic constraints associated with observing INS at small momentum transfers. Because it is equipped with a dedicated small-angle detector bank, HRC is capable of the so-called neutron Brillouin scattering (NBS) [21], that is, INS close to the forward direction [22]. A successful outcome of the NBS experiment is a study of spin-waves in the metallic ferromagnet $SrRuO_3$ [23]. In the said study, ferromagnetic spin-waves in a powder sample, which are difficult to observe by conventional INS because of the rapid decrease in scattering intensity as a function of Q, were observed by using NBS. The observed temperature dependence of the spin gap was related to anomalous Hall conductivity and was reproduced using the framework of Weyl fermions. Moreover, the NBS experiments conducted using HRC were quite effective from the viewpoint of studying the collective dynamics of liquids [24, 25].

2.3. AMATERAS

AMATERAS was designed for QENS and INS measurements in cold to sub-thermal neutron energy regions. In particular, high resolutions and fine line profiles can be obtained by

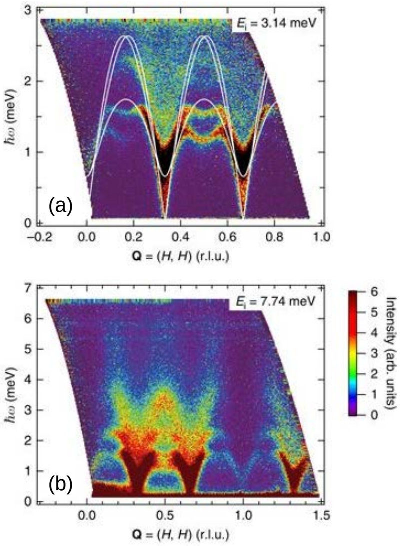

Figure 4: Magnetic excitation spectra of $Ba_3CoSb_2O_9$ at 1.0 K observed using AMATERAS with (a) E_i = 3.14 meV and (b) 7.74 meV. The figure is reproduced from Ref. [26].

using the pulse-shaping choppers. Fig. 4 shows a recent outstanding outcome in terms of the observation of the magnetic excitations in $Ba_3CoSb_2O_9$ [26]. By utilizing a set of E_is simultaneously [27, 28], AMATERAS could successfully explore the hierarchical structure of magnetic excitations in this $S = 1/2$ triangular-lattice Heisenberg antiferromagnet. The magnetic excitations were characterized by dispersive excitations and continuum scattering at low energies [Fig. 4(a)], whereas at high energies, they were dominated by a columnar continuum extending above 10 meV, six times larger than the exchange interaction [Fig. 4(b)]. This finding challenged theories related to the triangular-lattice quantum spin system.

As for QENS, a new analysis method to extract vibration modes from quasielastic scattering data was developed with this instrument [29]. This method, called mode-distribution analysis, assumes that the quasielastic scattering profile consists of arbitrary combinations of Lorentzian modes and determines the mode distributions without using information about the number of modes. This method was applied to analyze the QENS data of liquid water by Kikuchi et al., who revealed the existence of a new intermediate mode of the water molecule, in addition to the known fast and slow modes [29]. The dynamical structure factor obtained by quasielastic and inelastic scatterings can be Fourier-transformed to obtain the real-space structure factor or the real-time and real-space structure factor. This type of analysis is useful for obtaining information on local dynamical correlations [30, 31]. Kawakita et al. introduced a new procedure to deduce real-time and real-space dynamical structure factors of liquid bismuth, in which the maximum entropy method was used to prevent truncation errors in Fourier transforms due to the finite ranges of momentum transfers [32]. A similar approach was employed by Nakamura et al. to deduce real-space dynamical structure factors from the phonon spectra of polycrystalline NaI measured using 4SEASONS [33].

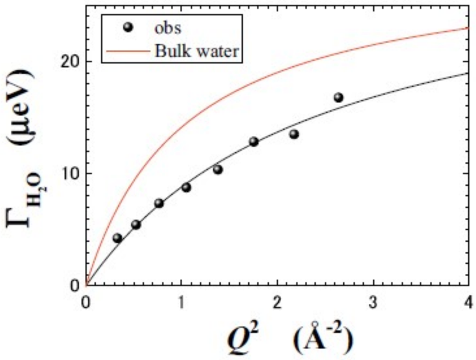

Figure 5: Q^2 dependence of HWHM of QENS profiles of water in water pocket observed at −20 ℃ by using DNA. The black line is the fitted values based on a jump-diffusion model, and the red line represents the values of bulk water at −20 ℃. The figure is reproduced from Ref. [35].

2.4. DNA

DNA can provide micro-eV energy resolution measurements over a broad energy range of $-500\,\mu\mathrm{eV} < E < 1500\,\mu\mathrm{eV}$, thanks to the near-backscattering geometry of the instrument and the pulse-shaping options. In addition, the high-efficiency and high signal-to-noise (S/N) ratio ($S/N \sim 10^5$) of the instrument facilitate measurements with small scattering amplitudes or with small quantities of samples (of the order of milligrams). The above-mentioned features were exploited to study the dynamics of human hemoglobin, which plays an important role in transporting O_2 from the lungs to tissues [34]. Fujiwara et al. measured the QENSs of two forms of hemoglobin, namely, deoxyhemoglobin and CO hemoglobin, with an energy resolution of 12 μeV. They found that the CO form involves internal large-scale motions in addition to translational and rotational diffusions of a rigid body. Another interesting example is the study of water in an ionic liquid [35]. Water in an ionic liquid 1-butyl-3-methylimidazolium nitrate ([C_4mim][NO_3]) forms a nano-domain structure called "water pocket," in which water is confined in nano-spaces. Abe et al. studied the dynamics of water in the water pocket by performing QENS measurements with an energy resolution of 3.6 μeV. Fig. 5 shows the half-widths-at-half-maximum (HWHMs) of the QENS spectra as a function of the square of momentum transfer (Q^2). It indicates that the dynamic behavior of water in the water pocket is slower than that of bulk water.

2.5. Annual trend

Fig. 6 shows the annual trends in the numbers of reviewed papers published based on the results obtained using the MLF spectrometers. The number of papers published based on the results obtained using 4SEASONS, HRC, and AMATERAS started to increase from around 2011. The numbers of papers published based on the results obtained using VIN ROSE and POLANO remain low, because the associated user programs are yet to commence or have commenced recently, and the existing papers are mostly technical reports of instrument development. Notably, the number of papers from DNA was low before 2016, but it increased suddenly since 2017. Seemingly, this younger

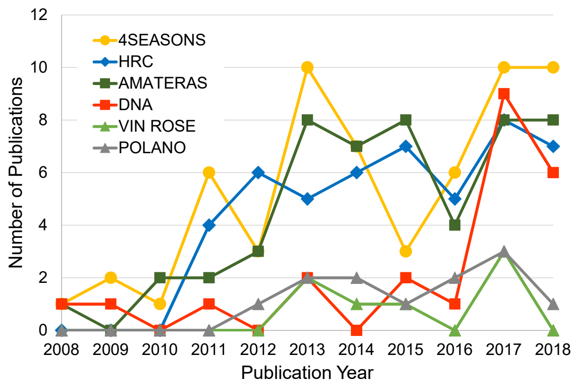

Figure 6: Annual trends of numbers of reviewed papers published based on results obtained from MLF spectrometers as of August 2018. The papers written in Japanese are excluded.

but potentially workhorse instrument is finally catching up to the former three instruments.

3. Developments related to MLF Spectrometers

3.1. Development of new instruments

VIN ROSE consists of two types of spin-echo instruments: MIEZE (Modulated Intensity with Zero Effort) and NRSE (Neutron Resonance Spin Echo) [9, 36, 37]. It can measure intermediate scattering functions directly by conducting neutron polarization analysis. VIN ROSE can be used to perform measurements with the highest energy resolution among the MLF spectrometers, and the TOF technique offers higher efficiency compared to its counterparts for steady sources. The most remarkable progress pertaining to this instrument is that the associated user program has finally commenced: the user program started partially with the MIEZE spectrometer since the 2017B proposal round. In addition, key components of the instrument have been upgraded. As for the MIEZE spectrometer, an 800-kHz MIEZE signal has been achieved [Fig. 7(a)]. This high-frequency signal corresponds to a Fourier time of as long as 15 nsec at a wavelength of 13 Å. In addition, the VIN ROSE group has developed a supermirror device for the NRSE spectrometer, which is used to correct the optical-path difference and is indispensable for achieving a high resolution [38]. This 90-cm-long spheroidal supermirror device consists of $m = 5$ supermirrors, and its focal length is 2.5 m. Fig. 7(b) shows one of the spheroidal supermirror pieces constituting the supermirror device, and Fig. 7(c) shows the neutron spin-echo signal observed using this supermirror device. The spin-echo signal is observed clearly over a wide wavelength region (0.67–1.62 nm). This result proves that the path-difference correction performed by the supermirror device is successful [39].

POLANO is dedicated to polarized neutron scattering over a very wide scattering angle. It is aimed at polarization analysis at energy transfers of up to 100 meV, which is higher compared to that in the case of conventional polarized neutron spectrometers. Such high-energy polarization analysis will be useful for studying, for example, the respective roles of phonons and magnons in high-critical-temperature superconductors. POLANO

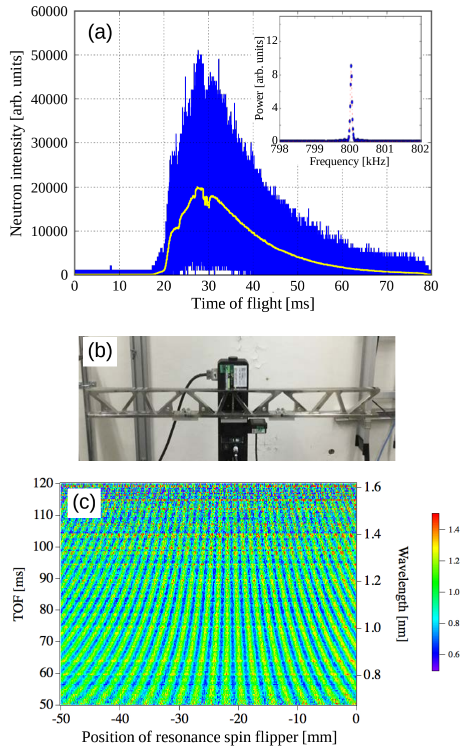

Figure 7: (a) Experimentally observed TOF-MIEZE signal at 800 kHz (blue line). The neutron TOF spectrum is superposed (yellow line). The inset shows the corresponding power spectrum obtained by Fourier transformation. (b) A piece of spheroidal supermirror for the NRSE spectrometer. (c) Neutron spin-echo signal observed with the supermirror device at the NRSE spectrometer. The left (right) horizontal axis denotes the neutron TOF (or wavelength), and the horizontal axis denotes the position of the downstream high-frequency resonant spin flipper.

was under construction until recently. The development of fundamental equipment for a conventional neutron spectrometer, such as detectors, a vacuum pumping system consisting of scroll pumps and cryopumps, and a chopper system, has been completed quite recently [40]. Then, on-beam commissioning of POLANO started in 2017. Fig. 8(a) shows the result of on-beam calibration of the detectors. It shows the neutron intensity distribution on the detector arrays when a white neutron beam is irradiated on an incoherent scatterer at the sample position [41]. The dark rectangle in the middle row indicates a beam stop located in the direct beam, and the bright horizontal lines on the detectors show projections of the cadmium slits surrounding the sample. The latter indicates that the positional parameters of the detectors are well determined. The POLANO group will start a user program without polarization analysis in 2019. By contrast, the group will develop the polarization system in a stepwise manner [42]. The target in the first phase is to perform polarization experiments with a final neutron energy of ~30 meV by using a combination of SEOP (spin exchange optical pumping)-type ^{3}He spin filter as the polarizer and a set of fan-shape bender mirrors as the analyzer. Development of the polarization devices for the phase-1 polarization experiments, including an *in situ* SEOP system, an analyzer on a movable

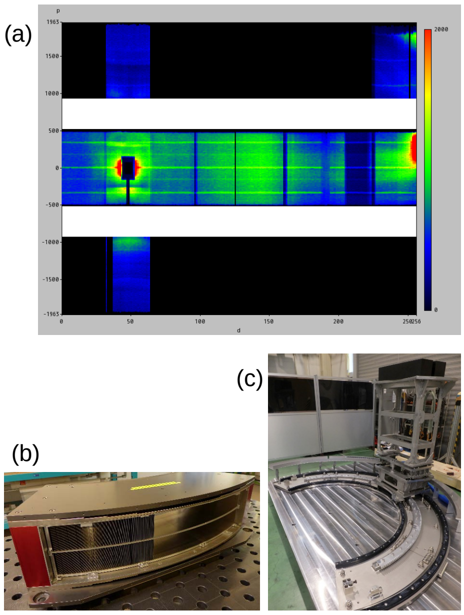

Figure 8: (a) Neutron intensities on the detector arrays of POLANO during detector calibration work. (b) Analyzer mirror of POLANO, and (c) its rotating system.

stage [Figs. 8(b) and 8(c)], and a guide field and Helmholtz coil system, is almost complete [41].

3.2. Developments related to instruments under operation

In addition to considerable progress in the development of the two above-described instruments, the other four instruments continue to be upgraded, even as their user programs remain operational. For example, in the case of 4SEASONS, AMATERAS, and DNA, the numbers of ^{3}He detectors (4SEASONS [16] and AMATERAS) or Si(311) analyzers (DNA) are being increased to expand their momentum transfer ranges in order to cope with the rising demand to measure lattice dynamics [43–48]. The HRC group focused on improving the performance of NBS measurements: they succeeded in increasing the intensity by a factor of 2.4 at an energy resolution (ΔE) $\Delta E/E_\mathrm{i} = 2\%$ by optimizing the geometrical parameters of the Fermi chopper and improving the design of the beam collimator and the configurations of the small-angle detectors [49]. Moreover, recently, they succeeded in further increasing the neutron intensity and achieving an energy resolution of nearly 1% [50].

Sample environments have become more important in recent neutron scattering facilities, and the development of sample environments is as important as the development of instruments. In MLF, the Sample Environment (SE) team has systematically introduced new devices and developed maintenance environments [51]. In parallel, the instruments are being prepared to employ these new devices or devices specific to each instrument are being developed. Recently, in the MLF spectroscopy group, the HRC group developed a piston-cylinder clamped cell for high-pressure experiments up to 1.5 GPa, which is mountable on their 1-K refrigerator. They succeeded in observing the pressure-induced quantum phase transition in the one-dimensional (1D) antiferromagnet $CsFeCl_3$ by using this pressure cell [52, 53]. The 4SEASONS group has estimated the magnitude of stray-field from the MLF-SE superconducting magnet and performed test measurements in order to prepare for actual use of the magnet [16, 54]. We developed an oscillating radial collimator for the MLF-SE superconducting magnet to reduce background scattering from the magnet. The collimator can be used in experiments at 4SEASONS, AMATERAS, and HRC, and it has already been used in four user experiments at AMATERAS. The DNA group has performed cooling tests of the MLF-SE ^{3}He cryostat and dilution refrigerator with a new 2-K cryostat because sub-K sample environments are indispensable for utilizing the fine energy resolution of DNA to study low-energy excitations. They confirmed the lowest temperatures of 300 mK (^{3}He) and 50 mK (dilution), which opened many doors in terms of high-resolution low-temperature measurements.

Some of devices installed on the instruments, unfortunately, do not perform as expected or their performance degrades over the years. Especially, the aging problem is becoming severe now that the facility has been operational for 10 years. Maintenance or replacement of the degraded devices is indispensable for stable operation of the instruments, and it is as important as the development of new devices. For example, we found that the fast disk choppers used in AMATERAS and DNA start vibrating unstably at high speeds, and we suspect some defects in the carbon fiber-reinforced plastic (CFRP) disks. This problem limits the maximum available speeds to 275 Hz, which is considerably lower than the designed value (350 Hz) [55]. Several of the unstable disks have been replaced recently, and the rest will be replaced in the near future. Similar problems have occurred in the Fermi choppers of 4SEASONS and HRC owing to the deformation of slit packages, and both have been replaced already. AMATERAS and HRC utilize large-capacity cryopumps to evacuate their large vacuum vessels and achieve cryogenic vacuum. Unfortunately, these cryopumps have malfunctioned repeatedly [55], and in both instruments the pumps were replaced with new units.

4. Glimpse of a 1-MW operation

On July 3, 2018, MLF succeeded in operating continuously at a beam power of approximately 1 MW. Given that this 1-MW operation was conducted for testing purposes, the continuous operation duration was only 1 h. Nevertheless, a few of the instruments in MLF were used to perform experiments in order to demonstrate their performance. Fig. 9 shows examples of such experiments performed using MLF spectrometers, which challenged short-time measurements of the magnetic excitation spectra in 1D Heisenberg antiferromagnets. Figs. 9(a)–(c) show magnetic excitations in a 0.5 cc single crystal of $CuGeO_3$, while Figs. 9(d) and 9(e) show magnetic excitations in a 0.3 cc single crystal of $KCuGaF_6$. The latter crystal is the same as that used in Ref. [56]. In both experiments, the crystals are aligned such that their 1D spin chains are perpendicular to the incident beam, and the scattering intensities collected for one minute are integrated along the other two axes. Even with these short-time measurements, characteristic spin-wave-like dispersions

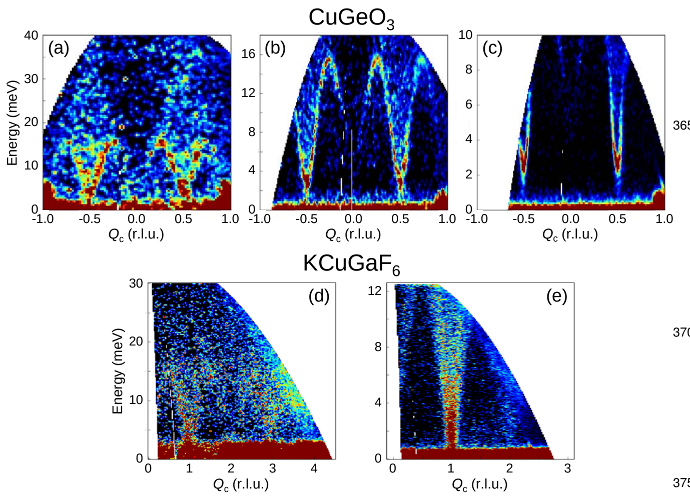

Figure 9: (a)–(c) Magnetic excitation spectra in $CuGeO_3$ observed at 5.8 K by using 4SEASONS with (a) E_i = 45 meV, (b) 22 meV, and (c) 13 meV. (d) and (e) Magnetic excitation spectra in $KCuGaF_6$ observed at 5.2 K by using AMATERAS with (d) E_i = 35 meV and (e) 14 meV. The data for one minute were extracted from event-recorded raw data by using the software package Utsusemi [15]. The datasets of (a)–(c) and (d) and (e) were obtained simultaneously by means of multi-E_i measurements.

and continuum excitations were captured [56, 57]. In particular, the intensity is stronger at lower incident energies. The features of the spin-wave-like excitations were observable even 10 s after starting the measurements. The high neutron flux proved by such experiments will not only lead to high measurement efficiency but also create new opportunities in QENS and INS experiments, such as *in situ* or time-transient experiments.

5. Summary

In this paper, we reviewed the present status of the neutron spectrometers in MLF of J-PARC. The MLF spectrometers consist of four direct-geometry, one inverted-geometry, and one spin-echo instruments, the last of which is subdivided into two different types of spectrometers. Now that the facility has been operational for 10 years, a number of interesting and important research outcomes have been produced from the four instruments that are open to users. Considerable progress has been made in the development of two new instruments, whereas the other instruments continue to be developed for higher flux, flexibility, and so on. In addition, we encountered the problems of aging and unsatisfactory performance in the cases of a few devices, and these problems have been or will be fixed. The results of test experiments with 1-MW beam power were highly promising from the viewpoint of the future of MLF spectrometers when the facility will reach the designed beam power.

Acknowledgments

We thank Dr. H. Hino and Dr. T. Oda for providing the elliptical supper mirrors and the 800-kHz MIEZE signal data, respectively. We thank Prof. H. Tanaka for providing the $KCuGaF_6$ single crystal. Development of the ellipsoid supermirror was supported by Photon and Quantum Basic Research Coordinated Development Program, MEXT, and Adaptable and Seamless Technology Transfer Program through Target driven R&D, JST. TY and the POLANO project are partly supported by Grant-in-Aid for Scientific Research (A) JP16H02125. The MLF experiment proposal numbers are 2014B0152, 2014S01, 2014S07, 2014S09, 2015S01, 2016S01, 2017I0002, 2017S01, 2018I0001, and 2018I0014.

References

[1] H. Takada, K. Haga, M. Teshigawara, T. Aso, S.-I. Meigo, H. Kogawa, T. Naoe, T. Wakui, M. Ooi, M. Harada, M. Futakawa, Materials and Life Science Experimental Facility at the Japan Proton Accelerator Research Complex I: Pulsed spallation neutron source, Quantum Beam Sci. 1 (2017) 8. doi:10.3390/qubs1020008.

[2] K. Nakajima, Y. Kawakita, S. Itoh, J. Abe, K. Aizawa, H. Aoki, H. Endo, M. Fujita, K. Funakoshi, W. Gong, M. Harada, S. Harjo, T. Hattori, M. Hino, T. Honda, A. Hoshikawa, K. Ikeda, T. Ino, T. Ishigaki, Y. Ishikawa, H. Iwase, T. Kai, R. Kajimoto, T. Kamiyama, N. Kaneko, D. Kawana, S. Ohira-Kawamura, T. Kawasaki, A. Kimura, R. Kiyanagi, K. Kojima, K. Kusaka, S. Lee, S. Machida, T. Masuda, K. Mishima, K. Mitamura, M. Nakamura, S. Nakamura, A. Nakao, T. Oda, T. Ohhara, K. Ohishi, H. Ohshita, K. Oikawa, T. Otomo, A. Sano-Furukawa, K. Shibata, T. Shinohara, K. Soyama, J. Suzuki, K. Suzuya, A. Takahara, S. Takata, M. Takeda, Y. Toh, S. Torii, N. Torikai, N. L. Yamada, T. Yamada, D. Yamazaki, T. Yokoo, M. Yonemura, H. Yoshizawa, Materials and Life Science Experimental Facility (MLF) at the Japan Proton Accelerator Research Complex II: Neutron scattering instruments, Quantum Beam Sci. 1 (2017) 9. doi:10.3390/qubs1030009.

[3] H. Seto, S. Itoh, T. Yokoo, H. Endo, K. Nakajima, K. Shibata, R. Kajimoto, S. Ohira-Kawamura, M. Nakamura, Y. Kawakita, H. Nakagawa, T. Yamada, Inelastic and quasi-elastic neutron scattering spectrometers in J-PARC, Biochim. Biophys. Acta, Gen. Subj. 1861 (2017) 3651–3660. doi:10.1016/j.bbagen.2016.04.025.

[4] R. Kajimoto, M. Nakamura, Y. Inamura, F. Mizuno, K. Nakajima, S. Ohira-Kawamura, T. Yokoo, T. Nakatani, R. Maruyama, K. Soyama, K. Shibata, K. Suzuya, S. Sato, K. Aizawa, M. Arai, S. Wakimoto, M. Ishikado, S. Shamoto, M. Fujita, H. Hiraka, K. Ohoyama, K. Yamada, C.-H. Lee, The Fermi chopper spectrometer 4SEASONS at J-PARC, J. Phys. Soc. Jpn. 80 (2011) SB025. doi:10.1143/JPSJS.80SB.SB025.

[5] S. Itoh, T. Yokoo, S. Satoh, S. ichiro Yano, D. Kawana, J. Suzuki, T. J. Sato, High Resolution Chopper Spectrometer (HRC) at J-PARC, Nucl. Instrum. Methods Phys. Res., Sect. A 631 (2011) 90 – 97. doi:10.1016/j.nima.2010.11.107.

[6] K. Nakajima, S. Ohira-Kawamura, T. Kikuchi, M. Nakamura, R. Kajimoto, Y. Inamura, N. Takahashi, K. Aizawa, K. Suzuya, K. Shibata, T. Nakatani, K. Soyama, R. Maruyama, H. Tanaka, W. Kambara, T. Iwahashi, Y. Itoh, T. Osakabe, S. Wakimoto, K. Kakurai, F. Maekawa, M. Harada, K. Oikawa, R. E. Lechner, F. Mezei, M. Arai, AMATERAS: A cold-neutron disk chopper spectrometer, J. Phys. Soc. Jpn. 80 (2011) SB028. doi:10.1143/JPSJS.80SB.SB028.

[7] T. Yokoo, K. Ohoyama, S. Itoh, J. Suzuki, K. Iwasa, T. J. Sato, H. Kira, Y. Sakaguchi, T. Ino, T. Oku, K. Tomiyasu, M. Matsuura, H. Hiraka, M. Fujita, H. Kimura, T. Sato, J. Suzuki, M. Takeda, K. Kaneko, M. Hino, S. Muto, Newly proposed inelastic neutron spectrometer POLANO, J. Phys. Soc. Jpn. 82 (2013) SA035. doi:10.7566/JPSJS.82SA.SA035.

[8] K. Shibata, N. Takahashi, Y. Kawakita, M. Matsuura, T. Yamada, T. Tominaga, W. Kambara, M. Kobayashi, Y. Inamura, T. Nakatani, K. Nakajima, M. Arai, The performance of TOF near backscattering spectrometer DNA in MLF, J-PARC, JPS Conf. Proc. 8 (2015) 036022. doi:10.7566/JPSCP.8.036022.

[9] M. Hino, T. Oda, N. L. Yamada, H. Endo, H. Seto, M. Kitaguchi, M. Harada, Y. Kawabata, Supermirror neutron guide system for neutron resonance spin echo spectrometers at a pulsed neutron source, J. Nucl. Sci. Technol. 54 (2017) 1223–1232. doi:10.1080/00223131.2017.1359699.

[10] K. Horigane, K. Kihou, K. Fujita, R. Kajimoto, K. Ikeuchi, S. Ji, J. Akimitsu, C. H. Lee, Spin excitations in hole-overdoped iron-based superconductors, Sci. Rep. 6 (2016) 33303. doi:10.1038/srep33303.

[11] M. Matsuura, S. Kawamura, M. Fujita, R. Kajimoto, K. Yamada, Development of spin-wave-like dispersive excitations below the pseudogap temperature in the high-temperature superconductor $La_{2-x}Sr_xCuO_4$, Phys. Rev. B 95 (2017) 024504. doi:10.1103/PhysRevB.95.024504.

[12] N. Murai, K. Suzuki, S. Ideta, M. Nakajima, K. Tanaka, H. Ikeda, R. Kajimoto, Effect of electron correlations on spin excitation bandwidth in $Ba_{0.75}K_{0.25}Fe_2As_2$ as seen via time-of-flight inelastic neutron scattering, Phys. Rev. B 97 (2018) 241112(R). doi:10.1103/PhysRevB.97.241112.

[13] K. Matsuura, H. Sagayama, A. Uehara, Y. Nii, R. Kajimoto, K. Kamazawa, K. Ikeuchi, S. Ji, N. Abe, T. Arima, Spin-orbital correlated dynamics in the spinel-type vanadium oxide MnV_2O_4, Phys. Rev. Lett. 119 (2017) 017201. doi:10.1103/PhysRevLett.119.017201.

[14] T. Kim, J. C. Leiner, K. Park, J. Oh, H. Sim, K. Iida, K. Kamazawa, J.-G. Park, Renormalization of spin excitations in hexagonal $HoMnO_3$ by magnon-phonon coupling, Phys. Rev. B 97 (2018) 201113(R). doi:10.1103/PhysRevB.97.201113.

[15] Y. Inamura, T. Nakatani, J. Suzuki, T. Otomo, Development status of software "Utsusemi" for chopper spectrometers at MLF, J-PARC, J. Phys. Soc. Jpn. 82 (2013) SA031. doi:10.7566/JPSJS.82SA.SA031.

[16] R. Kajimoto, M. Nakamura, Y. Inamura, K. Kamazawa, K. Ikeuchi, K. Iida, M. Ishikado, N. Murai, H. Kira, T. Nakatani, S. Ohira-Kawamura, R. Takahashi, N. Kubo, W. Kambara, K. Nakajima, K. Aizawa, Status report of the chopper spectrometer 4SEASONS, J. Phys.: Conf. Ser. 1021 (2018) 012030. doi:10.1088/1742-6596/1021/1/012030.

[17] Y. Inamura, T. Ito, J. Suzuki, Applications of the differential events reading method at MLF, J-PARC, J. Phys.: Conf. Ser. 1021 (2018) 012015. doi:10.1088/1742-6596/1021/1/012015.

[18] S. Hayashida, M. Soda, S. Itoh, T. Yokoo, K. Ohgushi, D. Kawana, H. M. Rønnow, T. Masuda, Magnetic model in multiferroic $NdFe_3(BO_3)_4$ investigated by inelastic neutron scattering, Phys. Rev. B 92 (2015) 054402. doi:10.1103/PhysRevB.92.054402.

[19] S. Ibuka, S. Itoh, T. Yokoo, Y. Endoh, Damped spin-wave excitations in the itinerant antiferromagnet γ-$Fe_{0.7}Mn_{0.3}$, Phys. Rev. B 95 (2017) 224406. doi:10.1103/PhysRevB.95.224406.

[20] M. Fujihala, H. Koorikawa, S. Mitsuda, K. Morita, T. Tohyama, K. Tomiyasu, A. Koda, H. Okabe, S. Itoh, T. Yokoo, S. Ibuka, M. Tadokoro, M. Itoh, H. Sagayama, R. Kumai, Y. Murakami, Possible tomonaga-luttinger spin liquid state in the spin-1/2 inequilateral diamond-chain compound $K_3Cu_3AlO_2(SO_4)_4$, Sci. Rep. 7 (2017) 16785. doi:10.1038/s41598-017-16935-9.

[21] S. Itoh, Y. Endoh, T. Yokoo, D. Kawana, Y. Kaneko, Y. Tokura, M. Fujita, Neutron Brillouin scattering with pulsed spallation neutron source —spin-wave excitations from ferromagnetic powder samples—, J. Phys. Soc. Jpn. 82 (2013) 043001. doi:10.7566/JPSJ.82.043001.

[22] R. Robinson, Neutron Brillouin scattering with chopper spectrometers, Physica B 156-157 (1989) 557–560. doi:10.1016/0921-4526(89)90730-8.

[23] S. Itoh, Y. Endoh, T. Yokoo, S. Ibuka, J.-G. Park, Y. Kaneko, K. S. Takahashi, Y. Tokura, N. Nagaosa, Weyl fermions and spin dynamics of metallic ferromagnet $SrRuO_3$, Nat. Commun. 7 (2016) 11788. doi:10.1038/ncomms11788.

[24] S. Itoh, T. Yokoo, D. Kawana, Y. Kaneko, Y. Tokura, M. Fujita, K. Yoshida, K. Saito, N. Inami, Y. Takeichi, K. Ono, Y. Endoh, Neutron Brillouin scattering experiments with pulsed neutrons on High Resolution Chopper Spectrometer HRC, J. Phys.: Conf. Ser. 502 (2014) 012043. doi:10.1088/1742-6596/502/1/012043.

[25] K. Yoshida, T. Yamaguchi, T. Yokoo, S. Itoh, Collective dynamics measurement of liquid methanol by inelastic neutron scattering, J. Mol. Liq. 222 (2016) 395–397. doi:10.1016/j.molliq.2016.07.038.

[26] S. Ito, N. Kurita, H. Tanaka, S. Ohira-Kawamura, K. Nakajima, S. Itoh, K. Kuwahara, K. Kakurai, Structure of the magnetic excitations in the spin-1/2 triangular-lattice heisenberg antiferromagnet $Ba_3CoSb_2O_9$, Nat. Commun. 8 (2017) 235. doi:10.1038/s41467-017-00316-x.

[27] M. Russina, F. Mezei, First implementation of repetition rate multiplication in neutron spectroscopy, Nucl. Instrum. Methods Phys. Res., Sect. A 604 (2009) 624–631. doi:10.1016/j.nima.2009.03.010.

[28] M. Nakamura, R. Kajimoto, Y. Inamura, F. Mizuno, M. Fujita, T. Yokoo, M. Arai, First demonstration of novel method for inelastic neutron scattering measurement utilizing multiple incident energies, J. Phys. Soc. Jpn. 78 (2009) 093002. doi:10.1143/JPSJ.78.093002.

[29] T. Kikuchi, K. Nakajima, S. Ohira-Kawamura, Y. Inamura, O. Yamamuro, M. Kofu, Y. Kawakita, K. Suzuya, M. Nakamura, M. Arai, Mode-distribution analysis of quasielastic neutron scattering and application to liquid water, Phys. Rev. E 87 (2013) 062314. doi:10.1103/PhysRevE.87.062314.

[30] M. Arai, A. Hannon, T. Otomo, A. Hiramatsu, T. Nishijima, Dynamic correlation function studies of the medium-range order in materials, J. Non-Cryst. Solids 192-193 (1995) 230–237. doi:10.1016/0022-3093(95)00440-8.

[31] T. Egami, S. Billinge, Underneath the Bragg Peaks—Structural Analysis of Complex Materials, 2nd Edition, Elsevier, 2012, Pergamon Materials Series, Vol. 16.

[32] Y. Kawakita, T. Kikuchi, Y. Inamura, S. Tahara, K. Maruyama, T. Hanashima, M. Nakamura, R. Kiyanagi, Y. Yamauchi, K. Chiba, S. Ohira-Kawamura, Y. Sakaguchi, H. Shimakura, R. Takahashi, K. Nakajima, Anomaly of structural relaxation in complex liquid metal of bismuth - dynamic correlation function of coherent quasi-elastic neutron scattering, Physica Bdoi:10.1016/j.physb.2017.12.037.

[33] M. Nakamura, T. Kikuchi, K. Kamazawa, Y. Kawakita, Phonon dynamics of NaI investigated by $G(r, E)$ analysis, Physica Bdoi:10.1016/j.physb.2017.12.057.

[34] S. Fujiwara, T. Chatake, T. Matsuo, F. Kono, T. Tominaga, K. Shibata, A. Sato-Tomita, N. Shibayama, Ligation-dependent picosecond dynamics in human hemoglobin as revealed by quasielastic neutron scattering, J. Phys. Chem. B 121 (2017) 8069–8077. doi:10.1021/acs.jpcb.7b05182.

[35] H. Abe, T. Yamada, K. Shibata, Dynamic properties of nano-confined water in an ionic liquid, J. Mol. Liq. 264 (2018) 54–57. doi:10.1016/j.molliq.2018.05.006.

[36] M. Hino, T. Oda, M. Kitaguchi, N. L. Yamada, H. Sagehashi, Y. Kawabata, H. Seto, Current status of BL06 beam line for VIN ROSE at J-PARC/MLF, Phys. Procedia 42 (2013) 136–141. doi:10.1016/j.phpro.2013.03.187.

[37] T. Oda, M. Hino, H. Endo, N. L. Yamada, Y. Kawabata, H. Seto, Observation of 400-kHz TOF-MIEZE signals, JPS Conf. Proc. in press.

[38] T. Hosobata, M. Hino, H. Yoshinaga, T. Kawai, H. Endo, Y. Yamagata, N. L. Yamada, S. Takeda, Precision mechanical design of 900 mm long ellipsoidal neutron-focusing supermirror for VIN ROSE at J-PARC/MLF, JPS Conf. Proc. in press.

[39] H. Endo, T. Oda, H. Hino, Current status of the neutron resonance spin echo spectrometer on BL06 "VIN ROSE" at MLF, J-PARC, Physica B this issue.

[40] T. Yokoo, K. Ohoyama, S. Itoh, K. Iwasa, N. Kaneko, M. Ohkawara, S. Tasaki, T. Ino, K. Taketani, K. Aizawa, T. Oku, H. Kimura, T. J. Sato, Progress on POLANO spectrometer for polarized neutron experiment, in: Proc. ICANS-XXI, 2016, pp. 330–338, JAEA-Conf 2015-002/KEK Proceedings 2015-7. doi:10.11484/jaea-conf-2015-002.

[41] T. Yokoo, Y. Ikeda, S. Itoh, M. Fujita, M. Ohkawara, N. Kaneko, T. Ino, S. Sugai, Polarized neutron spectrometer POLANO, its construction and commissioning, Physica B this issue.

[42] T. Yokoo, S. Itoh, N. Kaneko, M. Fujita, T. Ino, M. Ohkawara, K. Ohoyama, M. Sakaguchi, Ready to roll? time to launch POLANO, AIP Conf. Proc. 1969 (2018) 050001. doi:10.1063/1.5039298.

[43] M. Kofu, N. Hashimoto, H. Akiba, H. Kobayashi, H. Kitagawa, K. Iida, M. Nakamura, O. Yamamuro, Vibrational states of atomic hydrogen in bulk and nanocrystalline palladium studied by neutron spectroscopy, Phys. Rev. B 96 (2017) 054304. doi:10.1103/PhysRevB.96.054304.

[44] R. Kajimoto, M. Nakamura, N. Murai, S. Shamoto, T. Honda, K. Ikeda, T. Otomo, H. Hata, T. Eto, M. Noda, H. Kuwahara, T. Okuda, Elastic and dynamical structural properties of la and mn-doped $SrTiO_3$ studied by neutron scattering and their relation with thermal conductivities, Sci. Rep. 8 (2018) 9651. doi:10.1038/s41598-018-27984-z.

[45] B. Li, Y. Kawakita, Y. Liu, M. Wang, M. Matsuura, K. Shibata, S. Ohira-Kawamura, T. Yamada, S. Lin, K. Nakajima, S. F. Liu, Polar rotor scattering as atomic-level origin of low mobility and thermal conductivity of perovskite $CH_3NH_3PbI_3$, Nat. Commun. 8 (2017) 16086. doi:10.1038/ncomms16086.

[46] B. Li, H. Wang, Y. Kawakita, Q. Zhang, M. Feygenson, H. L. Yu, D. Wu,

K. Ohara, T. Kikuchi, K. Shibata, T. Yamada, X. K. Ning, Y. Chen, J. Q. He, D. Vaknin, R. Q. Wu, K. Nakajima, M. G. Kanatzidis, Liquid-like thermal conduction in intercalated layered crystalline solids, Nat. Mater. 17 (2018) 226–230. doi:10.1038/s41563-017-0004-2.

[47] K. Suekuni, C. H. Lee, H. I. Tanaka, E. Nishibori, A. Nakamura, H. Kasai, H. Mori, H. Usui, M. Ochi, T. Hasegawa, M. Nakamura, S. Ohira-Kawamura, T. Kikuchi, K. Kaneko, H. Nishiate, K. Hashikuni, Y. Kosaka, K. Kuroki, T. Takabatake, Retreat from stress: Rattling in a planar coordination, Adv. Mater. 30 (2018) 1706230. doi:10.1002/adma.201706230.

[48] C. H. Lee, A. Nishida, T. Hasegawa, H. Nishiate, H. Kunioka, S. Ohira-Kawamura, M. Nakamura, K. Nakajima, Y. Mizuguchi, Effect of rattling motion without cage structure on lattice thermal conductivity in $LaOBiS_{2-x}Se_x$, Appl. Phys. Lett. 112 (2018) 023903. doi:10.1063/1.5010373.

[49] S. Itoh, T. Yokoo, T. Masuda, H. Yoshizawa, M. Soda, M. Yoshida, T. Hawai, D. Kawana, R. Sugiura, T. Asami, Y. Ihata, Improvement for neutron Brillouin scattering experiments on High Resolution Chopper Spectrometer HRC, J. Phys.: Conf. Ser. 1021 (2018) 012028. doi:10.1088/1742-6596/1021/1/012028.

[50] S. Itoh, T. Yokoo, T. Masuda, S. Asai, H. Saito, D. Kawana, R. Sugiura, T. Asami, Y. Ihata, Progress in High Resolution Chopper Spectrometer HRC by improving collimator and Fermi chopper, Physica B this issue.

[51] S. Ohira-Kawamura, T. Oku, M. Watanabe, R. Takahashi, K. Munakata, S. Takata, Y. Sakaguchi, M. Ishikado, K. Ohuchi, T. Hattori, H. Kira, K. Sakai, T. Aso, Y. Yamauchi, S. Isomae, Sample environment at the J-PARC MLF, J. Neutron Res. 19 (2017) 15–22. doi:10.3233/JNR-170046.

[52] S. Hayashida, O. Zaharko, N. Kurita, H. Tanaka, M. Hagihala, M. Soda, S. Itoh, Y. Uwatoko, T. Masuda, Pressure-induced quantum phase transition in the quantum antiferromagnet $CsFeCl_3$, Phys. Rev. B 97 (2018) 140405. doi:10.1103/PhysRevB.97.140405.

[53] S. Hayashida, Ph.D. thesis (2018).

[54] R. Kajimoto, M. Ishikado, H. Kira, K. Kaneko, M. Nakamura, K. Kamazawa, Y. Inamura, K. Ikeuchi, K. Iida, N. Murai, S. Ohira-Kawamura, R. Takahashi, K. Aoyama, W. Kambara, Study for use of a superconducting magnet and the first inelastic neutron scattering experiment under magnetic fields at the 4SEASONS spectrometer, Physica B this issue.

[55] K. Nakajima, S. Ohira-Kawamura, T. Kikuchi, M. Kofu, Y. Kawakita, Y. Inamura, W. Kambara, K. Aoyama, D. Wakai, M. Harada, M. Ooi, Recent issues encountered by AMATERAS: A cold-neutron disk-chopper spectrometer, J. Phys.: Conf. Ser. 1021 (2018) 012031. doi:10.1088/1742-6596/1021/1/012031.

[56] I. Umegaki, H. Tanaka, N. Kurita, T. Ono, M. Laver, C. Niedermayer, C. Rüegg, S. Ohira-Kawamura, K. Nakajima, K. Kakurai, Spinon, soliton, and breather in the spin-$\frac{1}{2}$ antiferromagnetic chain compound $KCuGaF_6$, Phys. Rev. B 92 (2015) 174412. doi:10.1103/PhysRevB.92.174412.

[57] M. Arai, M. Fujita, M. Motokawa, J. Akimitsu, S. M. Bennington, Quantum spin excitations in the spin-peierls system $CuGeO_3$, Phys. Rev. Lett. 77 (1996) 3649–3652. doi:10.1103/PhysRevLett.77.3649.